NIH Public Access
Author Manuscript
Cell Physiol Biochem. Author manuscript; available in PMC 2014 April 26.

Published in final edited form as:
Cell Physiol Biochem. 2013 ; 31(0): . doi:10.1159/000350077.

Regulation of Renal Organic Anion Transporter 3 (SLC22A8) Expression and Function by the Integrity of Lipid Raft Domains and their Associated Cytoskeleton

Chutima Srimaroeng[a,b], **Jennifer Perry Cecile**[b,c], **Ramsey Walden**[b], and **John B. Pritchard**[b]

[a]Department of Physiology, Faculty of Medicine, Chiang Mai University, Chiang Mai, Thailand [b]Laboratory of Toxicology and Pharmacology, National Institute of Environmental Health Sciences, Research Triangle Park, NC, USA [c]Department of Chemistry, Appalachian State University, Boone, NC, USA

Abstract

Background/Aims—In humans and rodents, organic anion transporter 3 (Oat3) is highly expressed on the basolateral membrane of renal proximal tubules and mediates the secretion of exogenous and endogenous anions. Regulation of Oat3 expression and function has been observed in both expression system and intact renal epithelia. However, information on the local membrane environment of Oat3 and its role is limited. Lipid raft domains (LRD; cholesterol-rich domains of the plasma membrane) play important roles in membrane protein expression, function and targeting. In the present study, we have examined the role of LRD-rich membranes and their associated cytoskeletal proteins on Oat3 expression and function.

Methods—LRD-rich membranes were isolated from rat renal cortical tissues and from HEK-293 cells stably expressing human OAT3 (hOAT3) by differential centrifugation with triton X-100 extraction. Western blots were subsequently analyzed to determine protein expression. In addition, the effect of disruption of LRD-rich membranes was examined on functional Oat3 mediated estrone sulfate (ES) transport in rat renal cortical slices. Cytoskeleton disruptors were investigated in both hOAT3 expressing HEK-293 cells and rat renal cortical slices.

Results—Lipid-enriched membranes from rat renal cortical tissues and hOAT3-expressing HEK-293 cells showed co-expression of rOat3/hOAT3 and several lipid raft-associated proteins, specifically caveolin 1 (Cav1), β-actin and myosin. Moreover, immunohistochemistry in hOAT3-expressing HEK-293 cells demonstrated that these LRD-rich proteins co-localized with hOAT3. Potassium iodide (KI), an inhibitor of protein-cytoskeletal interaction, effectively detached cytoskeleton proteins and hOAT3 from plasma membrane, leading to redistribution of hOAT3 into non-LRD-rich compartments. In addition, inhibition of cytoskeleton integrity and membrane trafficking processes significantly reduced ES uptake mediated by both human and rat Oat3. Cholesterol depletion by methyl-β-cyclodextrin (MβCD) also led to a dose dependent reduction Oat3 expression and ES transport by rat renal cortical slices. Moreover, the up-regulation of rOat3-mediated transport seen following insulin stimulation was completely prevented by MβCD.

Copyright © 2013 S. Karger AG, Basel

Chutima Srimaroeng, Ph.D., Department of Physiology, Faculty of Medicine, Chiang Mai University, 110 Intavaroros Rd., Sri-phum district, Muang, Chiang Mai, 50200 (Thailand), Tel. 66-53-945-362, Fax 66-53-945-365, c.srimaroeng@gmail.com.

This is an Open Access article licensed under the terms of the Creative Commons Attribution-NonCommercial-NoDerivs 3.0 License (www.karger.com/OA-license), applicable to the online version of the article only. Distribution for non-commercial purposes only.

NIH-PA Author Manuscript
NIH-PA Author Manuscript
NIH-PA Author Manuscript

NIH-PA Author Manuscript

NIH-PA Author Manuscript

NIH-PA Author Manuscript

Conclusion—We have demonstrated that renal Oat3 resides in LRD-rich membranes in proximity to cytoskeletal and signaling proteins. Disruption of LRD-rich membranes by cholesterol-binding agents or protein trafficking inhibitors altered Oat3 expression and regulation. These findings indicate that the integrity of LRD-rich membranes and their associated proteins are essential for Oat3 expression and function.

Keywords

Renal organic anion transporter; Lipid rafts; Regulation; Transporters; Cytoskeleton

Introduction

Lipid raft domains (LRD) serve as platforms for cell surface signal transduction and protein targeting, regulation of membrane protein function, and modulation of cholesterol homeostasis [1, 2]. Caveolin (Cav), a structural protein component of caveolar-type lipid raft domains was shown to play functional roles in several cellular processes, including vesicular transport, cholesterol homeostasis, tumor suppression and intracellular signal transduction [1, 3, 4]. Several pathogens and toxins utilize caveolar endocytosis as a pathway to enter the host cells [1, 4]. Caveolin 1 (Cav1) is tightly bound to cholesterol and helps to regulate intracellular cholesterol concentration [5–7], and caveolar rafts serve as platforms for compartmentalization of signaling molecules, including muscarinic receptor associated Ca^{2+} signaling [8] and glucagon-like peptide stimulated extracellular signal regulated kinase 1 and 2 (ERK1/2) activation [9]. Recently, proteomic analysis also revealed a specific role for macrophage rafts in compartmentalization and regulation of the mitogen-activated protein kinase (MEK-ERK) signaling pathway [10]. In addition, cytoskeletal elements, including actin, tubulin, myosin, actinin and supervillin, have been shown to be enriched in LRD [11]. Here, they have been shown to be essential for the structural and functional characteristics of LRD. For example, depolymerization of microtubules by nocodazole attenuated Cav1 vesicle movement between the cell surface and specific endosomal compartments. Moreover, disruption of the actin cytoskeleton by latrunculin A resulted in extensive movement of intracellular Cav1 vesicles toward the microtubule containing centrosome [12]. Similarly, in Jurkat cells, co-treatment with the cholesterol binding agent, filipin, and the actin cytoskeleton disruptor, latrunculin B, interfered with co-clustering of raft-associated proteins and signaling cascade of the Src family of tyrosine kinases [13]. Thus, the function and regulation of other membrane proteins may be modulated via the integrity of LRD and their associated proteins. These include transporters. For instance, glycine transporter 1 (GLY1) was localized in a cholesterol-rich membrane domains of the Chinese hamster ovary K1 (CHO-K1) cells and the rate of glycine transport mediated by GLY1 was highly sensitive to membrane rafts integrity [14]. In renal epithelial cells, Na^+-H^+ exchanger 3 (NHE3) and Na^+-K^+-ATPase (NKA) were shown to associate with LRD and their functions were attenuated by cholesterol depletion [15, 16]. Moreover, organic anion transporter 1 (Oat1) and Cav2 were shown to co-localize in renal primary culture cells; whereas, Oat3 was co-expressed with Cav1. Decreasing expression of either Cav1 or Cav2 led to a reduction of Oat1 or Oat3 function [17, 18]. This study addressed protein-protein interactions and did not investigate the role of the caveolar-type lipid rafts in Oat1 and Oat3 function. Therefore, we examined the hypothesis that changes in LRD-rich membrane composition, induced by cellular membrane cholesterol content interference or by cytoskeletal proteins disruption may affect Oat3 expression and function, and lead to changes in the pharmacokinetics of the substrates, including drugs and xenobiotics.

This study is focused on the regulation and function of renal Oat3. As the most highly expressed OAT in human renal epithelial cells [19], Oat3 has been shown to play an important role in handling a broad variety of endogenous metabolites, drugs, and

NIH-PA Author Manuscript

NIH-PA Author Manuscript

NIH-PA Author Manuscript

xenobiotics including prostaglandin E_2 and $F_{2\alpha}$, adrenaline, serotonin, antibiotics, antivirals, anti-epileptics, anti-neoplastics, non-steroidal anti-inflammatory drugs and ochratoxin A [20–23]. An Oat3 knock-out mouse model has conclusively demonstrated that Oat3 also mediates transport of organic anions in liver and choroid plexus [24–27]. Thus, it is positioned to have a major impact on distribution and elimination of drugs and toxins in both barrier and excretory tissues. In addition, Oat3 was also regulated by several compounds. For instance, the PKC activator, phorbol-12-myristate-13-acetate (PMA), down-regulated Oat1 and Oat3 function through decreased expression of Oat1 and Oat3 at the plasma membrane [28, 29]. In contrast, insulin and epidermal growth factor (EGF) stimulated Oat1 and Oat3 function via increasing their expression at the plasma membrane [30]. In this study, we have 1) assessed the role of LRD-rich membranes and their associated proteins on expression and function of Oat3, 2) examined the association of LRD-rich membrane and Oat3 in human embryonic kidney 293 (HEK-293) cells stably expressing hOAT3 and rat renal cortical tissues, and 3) examined the impact of pharmacological manipulation of LRD-rich membrane integrity and Oat3 expression and function.

Materials and Methods

Chemicals

Polyclonal rabbit anti-rOat3 antibody was obtained from Cosmobio (Tokyo, Japan). Monoclonal mouse anti-β actin was purchased from Abcam (Cambridge, MA). Monoclonal anti-caveolin1 was purchased from Calbiochem (Billerica, MA). Polyclonal anti-myosin was purchased from Biomedical Technologies (Stoughton, MA). Anti-V5 and Alexa Fluor 488 goat anti-mouse and rabbit antibodies were obtained from Invitrogen (Carlsbad, CA). Human recombinant insulin, glutarate, methyl-beta-cyclodextrin (MβCD), alpha-cyclodextrin (α-CD), cycloheximide, brefeldin A (BFA), latrunculin A, okadaic acid and CelLytic™ MT mammalian tissue lysis/extraction reagent were obtained from Sigma Aldrich (St. Louis, MO). Complete protease inhibitor cocktail was purchased from Roche Applied Science (Indianapolis, IN). Tritiated estrone sulfate ([^{3}H]-ES; specific activity (SA) 50 Ci/mmol) was obtained from PerkinElmer Life Sciences (Boston, MA). Tetra-ethylammonium bromide ([^{14}C]-TEA; SA 55 mCi/mmol) and 1-methyl-4-phenylpyridinium ([^{3}H]-MPP$^+$; SA 1 mCi/mmol) were obtained from American Radiolabled Chemicals (St. Louis, MO). All other chemicals were purchased from commercial sources at the highest purity available.

Animals

Adult male Sprague Dawley rats were euthanized by either CO_2 or pentobarbital followed by decapitation according to protocols approved by the National Institute of Environmental Health Sciences (NIEHS) and Chiang Mai University Animal Care and Use Committees. Kidneys were excised and placed in oxygenated saline buffer for experimental use. Animals were given standard pelleted chow and water *ad libitum* and maintained on a 12-hrs light/dark cycle. The animals were fasted overnight prior to tissue harvest.

Detergent extraction of cell membranes

Renal cortical slices (≤0.5 mm; 5 – 15 mg, wet weight) were cut with a Stadie-Riggs microtome. To increase yields of the fractions, LRD-rich and non-LRD-rich membrane fractions were then prepared using a modification of the method previously described by Lockwich et al. [8]. Briefly, slices were suspended in CelLytic™ MT mammalian tissue lysis/extraction reagent containing 1% protease inhibitor according to the manufacturer's protocol. Tissues were then homogenized and centrifuged at 2,500 g for 10 min at 4°C and supernatant was re-suspended in a sucrose buffer containing (mM): 250 sucrose, 10 Tris-HEPES (pH.7.4), 1 DTT, and 1% protease inhibitor. The homogenate was centrifuged at

NIH-PA Author Manuscript

NIH-PA Author Manuscript

NIH-PA Author Manuscript

3,000 g for 15 min at 4°C. The supernatant was then centrifuged at 50,000 g for 30 min at 4°C. The supernatant fraction from this spin was designated as the cytoplasmic fraction (C). The crude membrane pellets were re-suspended in a sucrose buffer and extracted for 1 hr at 4°C in a lysis buffer containing (mM): 50 Tris-HCl (pH.7.5), 150 NaCl, 5 EDTA and 1% triton X-100 (v/v). Samples were then centrifuged at 4°C for 1 hr 30 min at 100,000 g. The supernatant fraction was designated as the soluble, or non-LRD-rich, fraction (S). The pellets were re-suspended in the lysis buffer and designated as the insoluble fraction (I), or LRD-rich fraction. All samples (C, S, I) were stored at –80°C prior to use.

A HEK-293 cell line stably expressing hOAT3 with a V5 tag was generated previously [31] using pEF/FRT/V5-DEST vector. LRD-rich membranes were isolated from these cells using a modification of the method previously described by Lockwich et al. [8]. Cells were washed two times with cold phosphate-buffered saline (PBS) and suspended in CelLytic™ MT mammalian tissue lysis/extraction reagent containing 1% protease inhibitor. Cells were then homogenized and centrifuged at 250 g for 10 min at 4°C and the supernatant was re-suspended in a sucrose buffer and extracted for 1 hr at 4°C in a lysis buffer containing (mM): 50 Tris-HCl (pH.7.5), 150 NaCl, 5 EDTA and 1% triton X-100 (v/v). To disrupt cytoskeleton protein interactions, 1 M KI was added to the lysis buffer in this step. Samples were then centrifuged at 4°C for 1 hr 30 min at 100,000 g and all fractions (C, S, I) were obtained as described above.

Immunostaining

Wild type (WT) and HEK-293 cells transfected with hOAT3-V5 tag were seeded on poly-D-lysine coated slides at a concentration of 1×10^5 cells/well and grown for 48 hrs at 37°C. Cells were then washed 3 times in Tris-buffered saline (TBS) and fixed in 3.8% formaldehyde for 10 min. Subsequently, cells were washed in TBS 3 times and permeabilized with 0.1% triton X-100 for 1 min. Cells were washed again for 3 times with TBS and incubated with blocker BSA (Pierce, Rockford, IL) for 30 min. Primary antibodies (see figure legends) were applied for 1 hr. Cells were then washed 3 times with TBS and incubated with a corresponding secondary antibody (Molecular Probes, Carlsbad, CA) for 1 hr and again washed 3 times with TBS. Images were taken with Argon ion 488 nm and HeNe 543 nm excitation using laser scanning confocal microscopy (Zeiss 510 NLO, Thornwood, NY).

Western Blot analysis

Protein content was measured using the Bradford assay (Biorad, Hercules, CA). For each sample, 50 μg were heated in 4X NuPAGE® LDS sample buffer (Invitrogen, Carlsbad, CA) for 10 min. Invitrogen NuPAGE® Novex Bis-tris or 7% polyacrylamide gel was electrophoresed on an Invitrogen XCell Surelock (Grand Island, NY) or a Biorad apparatus (Hercules, CA). Polyvinylidene difluoride membranes were blocked for 1 hr with Pierce Starting Block PBS buffer (Rockford, IL) at 4°C and incubated overnight with a specific primary antibody (see figure legends). Membranes were washed with PBS-tween and incubated with a corresponding secondary antibody for 1 hr at 4°C. Supersignal West Pico chemiluminescent substrate (Pierce, Rockford, IL) was used to detect bands with a Gel doc XR™ system (Biorad, Hercules, CA).

Renal slice preparation and uptake study

After the rat kidneys were removed and placed in oxygenated saline buffer, renal cortical slices (≤0.5 mm; 5–15 mg, wet weight) were cut with a Stadie-Riggs microtome and maintained in ice-cold oxygenated modified Cross and Taggart buffer containing (mM): 95 NaCl, 80 mannitol, 5 KCl, 0.74 $CaCl_2$ and 9.5 Na_2HPO_4, pH 7.4). The slices were pre-incubated in 1 ml of buffer in the absence or presence of test compounds (see figure

NIH-PA Author Manuscript

NIH-PA Author Manuscript

NIH-PA Author Manuscript

legends) for 30 min and then incubated in 1 ml of buffer containing either 100 nM [^{3}H]-ES, 10 μM [^{14}C]-TEA or 1.25 nM [^{3}H]-MPP$^+$ for 30 min. Uptake was stopped by the addition of ice-cold buffer. Slices were washed, blotted, weighed, dissolved in 1 ml of 1 N NaOH and neutralized with 1 ml of 1 N HCl. Scintillation fluid of 15 ml was added and the radioactivity was measured using a Liquid Scintillation Analyzer (Packard, Meriden CT, USA). Uptake of radiolabeled substrate was calculated as tissue to medium (T/M) ratio, i.e., (DPM/g tissue)/(DPM ml medium).

Measurement of estrone sulfate transport in HEK-293 transfected hOAT3

HEK-293 WT and hOAT3-V5 transfected cell lines were seeded in 24-well poly-D-lysine coated tissue culture plates at a cell density of 2×10^5 cells/well. After culturing for 2 days, uptake experiments were performed at 37°C. The cells were first washed twice with 0.5 ml of Hanks' Balanced Salt Solution (Sigma Aldrich, St. Louis, MO) buffered with 10 mM HEPES (HBSS-HEPES), and pre-incubated in the same solution for 10 min. The cells were then pre-incubated in 0.5 ml of HBSS-HEPES solution for 30 min in the absence or presence of test compounds (see figure legends) and incubated with 0.3 ml of 100 nM [^{3}H]-ES for 5 min. Uptake was stopped by the addition of ice-cold HBSS-HEPES solution, and the cells were washed two times with the same solution. The cells in each well were lysed with 0.5 ml of 1 N NaOH, and neutralized with 0.5 ml of 1N HCl. Radioactivity was measured after the addition of scintillation fluid and detected by a Tri-Carb™ 2900 TR Liquid Scintillation Analyzer (Packard, Meriden CT, USA).

Statistical analysis

Data were expressed as mean ± S.D. Statistical differences were assessed using unpaired, two-tailed Student's t-test in GraphPad Prism (La Jolla, CA). Differences were considered to be significant at *, $p<0.05$, **, $p<0.01$, ***, $p<0.001$ versus control.

Results

OAT3 associated with lipid raft domains

To assess whether OAT3 resides in LRD-rich membranes, this insoluble fraction was isolated from rat renal cortex, and from a HEK-293 cell line transfected with a V5-tagged hOAT3 construct [31], using non-ionic detergent (1% triton X-100) according to a published methods [8]. A significant fraction of rOat3 from isolated renal cortex was associated with the insoluble (I) fraction, i.e. the LRD-rich fraction, with an apparent rOat3 molecular weight of ~150 kDa as detected by Western blot following gel electrophoresis. Additional rOat3 was recovered in the non-LRD-rich (S) fraction at a slightly lower molecular weight of ~130 kDa (Fig. 1A). LRD-associated cytoskeletal proteins, myosin and β-actin were also present in the insoluble fraction. Cav1, an integral protein marker for caveolae-type LRD membrane that had been shown previously to interact with Oat3 [18], was predominantly expressed in the LRD-rich fraction. Myosin was present in LRD-rich fraction, but was also expressed in cytosolic fraction. β-actin was present in both LRD- and non-LRD-rich fractions from rat renal cortical tissue (Fig. 1A). LRD from hOAT3 expressing HEK-293 cells were also detergent extracted and separated by SDS-PAGE. As shown in the Western blot in Figure 1B, human OAT3 was found mainly in an insoluble (I) fraction, as was Cav1, indicating the association of OAT3 and LRD-rich membrane was similar to that observed for rOat3 isolated from rat renal cortex. Next, the HEK-293 expressed hOAT3 cell extract was treated with KI, previously shown to disrupt cytoskeletal protein association with LRD [8]. Similar to myosin, when cytoskeletal protein localization in the LRD-rich fraction was disrupted by KI treatment, hOAT3 and Cav1 were re-distributed to soluble (S) and cytoplasmic fractions (Fig. 1B), suggesting that hOAT3 was associated with LRD-rich membrane and this association was lost upon disruption of the cytoskeleton.

NIH-PA Author Manuscript

NIH-PA Author Manuscript

NIH-PA Author Manuscript

Co-localization of Oat3 and raft-associated proteins

It was previously shown that Cav1 co-localized with rOat3 [18]. Therefore, immunofluorescence staining of anti-V5 tag for hOAT3, Cav1, myosin, and β-actin was conducted in the hOAT3-V5 expressing cells. As shown in Figure 2, hOAT3-V5 was mainly localized in the plasma membrane. There was also minor amorphous distribution within the intracellular compartment (Fig. 2A, D, G). The expression of the cytoskeletal markers, myosin (Fig. 2B) and β-actin (Fig. 2E), was seen throughout the cells; whereas, LRD marker, Cav1 (Fig. 2H), was highly expressed on the plasma membrane. Finally, as shown in the overlays, Cav1 and hOAT3 were co-localized, consistent with hOAT3 resides in caveolae-LRD (Fig. 2C, F, I, arrows).

Lipid raft-associated cytoskeleton is important for OAT3 function

As seen in Figures 1 and 2, a significant portion of both human and rat Oat3 resided in caveolar-type LRD-rich fraction. Since the cytoskeleton is an important component of functional LRD [12, 13], we assessed the importance of cytoskeleton proteins for Oat3 transport using both rat renal cortical slices and hOAT3-expressing HEK-293 cells. Rat Oat3 function was significantly reduced after the slices were pre-incubated with cycloheximide, a protein trafficking inhibitor (Fig. 3A). Brefeldin A (vesicle transport inhibitor), latrunculin A (actin depolymerizer), and okadaic acid (stimulate caveolae internalization), and a high concentration of myosin light chain kinase inhibitor 7 (100 μM, data not shown) also reduced ES transport, but these effects did not reach statistical significance (Fig. 3A). In hOAT3-expressing HEK-293 cells, pre-treatment with cycloheximide, brefeldin A, and latrunculin A for 30 min significantly inhibited ES uptake; whereas, okadaic acid and cytochalasin D (50 mg/ml, data not shown) did not change hOAT3 activity (Fig. 3B). These findings indicated that Oat3 function was reduced upon disruption of the cytoskeleton.

Cholesterol depletion by methyl-β-cyclodextrin (MβCD) specifically impaired Oat3 function mediated ES transport

To determine the role of the membrane lipid environment on Oat3 transport, rat cortical slices were pre-treated with three concentrations of the cholesterol depleting agent, methyl-β-cyclodextrin (MβCD), and uptake of 100 nM [^{3}H]-ES uptake was measured. As shown in Figure 4A, 5 and 10 mM MβCD significantly reduced ES uptake, while 1 mM MβCD had a little effect. Moreover, α-cyclodextrin (α-CD), an analog of MβCD ineffective in cholesterol depletion, did not significantly alter ES uptake at 10 mM. Together these data indicate that basal Oat3 transport requires the presence of cholesterol-rich LRD.

As a control to assess the general toxic effects of these agents on rat renal cortical slices, we examined their effects on organic cation transport under identical conditions. As shown in Figure 4B, the uptake of 10 μM [^{3}H]-TEA, a well transported substrate for organic cation transporters (Octs), was not significantly altered. We also addressed the impact of cholesterol depletion on [^{3}H]-MPP$^+$ substrate and used a potent Octs inhibitor, tetrapentylammonium (TPeA) to represent TPeA-sensitive Oct transport. As shown in Figure 4C, 1, 5, and 10 mM MβCD treatment significantly reduced [^{3}H]-MPP$^+$ uptake at the same extent (left panel). In contrast, neither 100 μM nor 1 mM of TPeA-sensitive MPP$^+$ uptake had shown the effect of cholesterol depletion by MβCD mediated by rOcts (middle and right panels). Hence, it appeared that the integrity of membrane lipid, particularly LRD-rich membrane, has a high impact for Oat3 transport of substrates, but not for Octs transport of substrates.

The observed decrease in Oat3 transport following manipulation of LRD integrity (Figs. 3 and 4) could be due to a decrease in transporter activity or a reduction in its surface expression, e.g. via altered trafficking to and from the membrane. In Figure 5A, as in Figure

NIH-PA Author Manuscript

NIH-PA Author Manuscript

NIH-PA Author Manuscript

1, rOat3 was mainly expressed in LRD-rich (I) fraction along with myosin, β-actin and Cav1 under control conditions. In addition, rOat3 was also seen in non-LRD-rich (S) and, to a lesser extent, in the cytoplasmic (C) fractions. After 10 mM MβCD exposure to deplete membrane cholesterol, rOat3 associated with the LRD-rich membranes was significantly decreased, rOat3 in non-LRD-rich fraction was unchanged, and cytosolic rOat3 was much higher. Detection of rOat3 bands in control and MβCD treated samples was quantitated by densitometry. The amount of rOat3 in each fraction was normalized by the amount of β-actin present in each respective fraction as shown in Figure 5B. The presence of 10 mM MβCD induced cholesterol dependent redistribution of rOat3 into cytosolic pool (Fig. 5B). However, β-actin and myosin distributions were unaffected by MβCD. Hence, this data indicated that LRD-rich membrane integrity was important for basal rOat3 function through the surface expression of rOat3.

Insulin stimulated ES transport mediated by Oat3 was abolished after removing membrane cholesterol

To determine whether the effect of cholesterol depletion had altered regulation of Oat3, we examined its effect on insulin-mediated stimulation of Oat3 activity. We had previously shown that insulin stimulated Oat3 function through PKCζ activation [32]. As shown above, 10 mM MβCD significantly reduced rOat3 expression and function, but 1 mM MβCD did not (Figs. 4A and 5A). Likewise, 30 min incubation of 1 mM MβCD did not change rOat3 expression in LRD-rich fraction (Fig. 6A). However, insulin mediated up-regulated rOat3 function was completely blocked by 1 mM MβCD; whereas, 1 mM α-CD did not prevent the stimulatory effect of insulin. Interestingly, the addition of 10 mM MβCD not only abolished the insulin effect, but also substantially inhibited rOat3 transport (Fig. 6B). Together, these results indicated that LRD-rich membrane have a significant role in rOat3 regulation, probably through altered trafficking of Oat3 to the plasma membrane.

Discussion

Renal Oat3 is highly expressed in the basolateral membrane of the proximal tubular epithelium where it plays a major role in the secretion of anionic metabolites and xenobiotics [19]. In the present study, we have examined the role of caveolae-type LRD-rich membrane on Oat3 function. Caveolae-type LRD exist in many cell types and are important in membrane protein targeting, sorting, signaling cascades, and compartmentalization [32, 33]. For example, it has been shown that insulin receptors are localized in caveolar domains of adipocytes plasma membranes and regulate their ability to transport glucose [34]. Moreover, disruption of caveolae-LRD integrity attenuated this transport. Such findings have led to the suggestion that perturbation of the structure and composition of LRD contributes to development of several human diseases, including cancer, cardiovascular, Alzheimer's, and chronic metabolic diseases [35]. In addition, LRD associated proteins, particularly cytoskeletal proteins, are important for membrane protein movement and expression [11, 36]. Disruption of microtubules and microfilaments by either nocodazole or latrunculin A abolished Cav1 vesicle trafficking in CHO expressed Cav1 cells [12], suggesting that agents altering LRD and associated structural proteins could affect membrane trafficking, localization, and function of transporters expressed there.

To assess this possibility for renal organic anion transport, we isolated detergent-resistant membrane domains or LRD-rich fraction from rat renal epithelium and HEK-293 cells expressing hOAT3 and investigated 1) whether there was any association between LRD-rich membranes and Oat3, and 2) the impact of LRD integrity on Oat3 function and regulation. As shown in Figures 1 and 2, Oat3 was associated with LRD-rich membranes in both rat kidney and hOAT3-expressing HEK-293 cells, as were Cav1 and LRD-associated cytoskeletal proteins. The association of Oat3 with LRD-rich membranes was similar to that

NIH-PA Author Manuscript

NIH-PA Author Manuscript

NIH-PA Author Manuscript

seen for other basolateral renal transporters including NKA and epithelial Na^+ channel (ENaC) in renal thick ascending limb and distal tubule, respectively [16, 37]. In addition, the apical NHE3 was also seen in LRD of renal proximal tubule [15]. Together, these finding indicate that Oat3, like other renal transporters, was physically located in LRD-rich membrane. However, it should be noted that rOat3 migrated as 150 kDa and 130 kDa, whereas, hOAT3 was detected at 75 kDa. The basis for this observation remains unclear, but it might be indicated the existence of membrane transporter oligomerization and/or membrane protein and its partner protein complexes. Previously, the major form of hOAT1 was seen at 360 kDa, suggesting that homo-oligomers of hOAT1 were present, since monomeric hOAT1 (~ 80 kDa) was not detected in hOAT1-myc-expressing LLC-K1 cells using gel filtration chromatography analysis. Moreover, similar to our finding, 1% triton X-100 did not change oligomeric states of hOAT1 [38]. Likewise, in previous studies rOat3 was observed at various molecular weights from 50–130 kDa depending on its source, antibody specificity, and treatments [18, 39, 40]. Our previous study also found rOat3 at 130 kDa associated with PKCζ, a binding protein, using co-immunoprecipitation [30]. Since Cav1 (21 kDa), a protein residing in the detergent-resistant fraction [32], was also found in rat kidney tissues [18], it is possible that an rOat3-Cav1 complex was present in detergent-resistant fraction (at 150 kDa); whereas, rOat3 oligomerization (at 130 kDa) exists in the soluble fraction. However, this remains speculative at present and the structural nature of rOat3 on the basolateral membrane of the kidney needs further investigation.

As shown in Figure 3, disruption of the integrity of LRD-rich membranes by either cytoskeleton disruptors (LTA) or protein trafficking inhibitors (cycloheximide and BFA) could interfere both rat and human Oat3 function. These findings were similar to previously seen for nocodazole inhibition of organic anion transport in teleost fish proximal tubule [41] that resulted, at least in part, from disruption of LRD-rich membrane integrity. Furthermore, nocodazole and BFA were suggested to decrease the up-regulation of Oat3 by insulin in rat renal cortical slices [30]. This finding is also consistent with the observation that disruption of cytoskeletal integrity after prolonged incubation of rat renal slices reduced rOat1 and 3 expression and function [42]. Of course, none of these findings preclude other mechanisms that may regulate Oat expression and function without interfering with LRD integrity. For instance, okadaic acid, a phosphatase inhibitor previously shown to promote caveolae internalization [32], was shown to phosphorylate mOat1, resulting in reduced mOat1 function [43]. Moreover, hOAT1 and hOAT3 mediated transport were decreased through the activation of PKC by PMA [29, 44, 45]. However, our current findings indicate that Oat3 expression and function is at least partly controlled by the integrity of LRD and associated cytoskeletal proteins in renal tubular epithelium.

Since both the structure and function of LRD-rich membrane depend upon the presence of cholesterol [1, 2], we examined the effects of cholesterol depletion on Oat3 expression and function (Figs. 5 and 6). MβCD was used to extract cholesterol from LRD-rich membrane *in vitro* [14, 46]. As shown in Figure 5, MβCD inhibited ES transport mediated by rOat3 in a dose-dependent manner, but did not inhibit Oct mediated-TEA transport in the same preparation. In addition, MβCD had an inhibitory effect on MPP^+ transport, it did not alter TPeA-sensitive component mediated by rOcts (Fig. C, *middle and right panels*). Thus, although Oct transporters had previously been observed in LRD fraction from rat kidney homogenate using tandem mass spectrometry [16], in contrast to rOat3-mediated ES transport, cholesterol depletion had less impact on rOcts-mediated substrate transport. This finding parallels previous data showing that MβCD treatment altered NHE3 activity, but not that of sodium glucose co-transporter 1 (SGLT1) [15]. Likewise, MβCD affected transport via glycine transporter 1, but not via transporter 2 [14]. Treatment of rat renal slices with 5 and 10 mM MβCD decreased rOat3 expression in LRD-rich fraction and promoted its redistribution into the cytosolic fraction (Fig. 5). A lower dose of MβCD (1 mM) did not

NIH-PA Author Manuscript

NIH-PA Author Manuscript

NIH-PA Author Manuscript

significantly alter rOat3 distribution. A similar dose dependent release of cholesterol had been seen previously in fibroblasts (60% and 90% after pre-incubation with 2 and 10 mM of MβCD) [46]. Such a shift in expression of transporters from LRD to non-LRD had also been reported for NKA [16] and the apical $Cl^-/HCO_3^-(OH^-)$ exchanger [47]. Moreover, the mobility of Cav1 was controlled by cholesterol content and intact cytoskeleton in Hela cell expressing Cav1 [48]. Similarly, our data revealed that Cav1 expression was nearly unchanged in the insoluble fraction, in contrast to rOat3 expression under cholesterol disruption (Fig. 5A). However, Cav1 re-distributed after KI treatment as shown in Fig. 1. Therefore, the actual mobility of Cav1 in complex tissues remains uncertain. Taken together, these data clearly indicate that integrity of LRD-rich membrane and associated cytoskeletal proteins had a significant impact on basal rOat3 localization and function.

Finally, as shown in Figure 6, cholesterol depletion of LRD-rich membrane also altered rOat3 regulation. Specifically, both 1 and 10 mM MβCD completely blunted the stimulatory effect of insulin on ES uptake via rOat3. Once again, these results parallel previous reports for other pathways. For example, insulin receptors were associated with caveolar rafts, and its signaling cascade was attenuated by β-cyclodextrin in isolated adipocytes [34]. Likewise, activation of cytosolic SGK1 stimulated ENaC activity, and this effect was abolished by MβCD in outside-out macropatches from *Xenopus Laevis* oocytes [37]. In contrast, the inactive cyclodextrin analog, α-CD, which does not effectively extract membrane cholesterol, was without effect on either basal function or insulin-stimulated rOat3 up-regulation. Interestingly, as shown in Figure 6B, 1 mM MβCD completely abolished rOat3 up-regulation without changing basal levels of transport in the absence of insulin, suggesting that this agent may prevent trafficking of Oat3 to the membrane at concentrations that do not lead to a redistribution of membrane associated Oat3 to the interior of the cell. Certainly, previous studies also suggest that LRD may control multiple aspects of signaling and compartmentation, e.g., insulin signaling in adipocytes [34], the Src family kinases actions in Jurkat cells [13] and MEK-ERK signaling cascade in intact macrophages [10].

In summary, we have demonstrated that integrity of LRD and its associated proteins may markedly alter Oat3 expression and function in kidney tissue and HEK-293 cells. These data suggest that Oat3 is localized in LRD-rich membrane along with cytoskeletal proteins, including β-actin and myosin. Expression and function of Oat3 was inhibited by cholesterol depletion of LRD-rich membrane by MβCD or by disruption of cytoskeletal proteins. Moreover, LRD-rich membrane disruption had a major impact on regulation of Oat3 function.

Acknowledgments

We wish to thank Drs. Timothy Lockwich for kindly providing detergent extraction of cell membrane protocol and Amy Aslamkhan for valuable suggestion in this manuscript. We also thank Mr. Chaya Vaddhanaphuti and Ms. Atcharaporn Ontawong for their assistance with manuscript preparation. This research was supported by the Faculty of Medicine Endowment Fund, Faculty of Medicine, Chiang Mai University, Chiang Mai, Thailand and the Intramural Research Program of the NIH, National Institute of Environmental Health Sciences, Research Triangle Park, NC, USA.

Abbreviations

LRD	lipid raft domain
Oat3	organic anion transporter 3
hOAT3	human organic anion transporter 3
rOat3	rat organic anion transporters 3

NIH-PA Author Manuscript

NIH-PA Author Manuscript

NIH-PA Author Manuscript

rOat1	rat organic anion transporters 1
ES	estrone sulfate
Cav1	caveolin 1
ERK1/2	extracellular signal regulated kinase
MEK-ERK	mitogen-activated protein kinase
KI	potassium iodide
MβCD	methyl-β-cyclodextrin
GLY1	glycine transporter 1
CHO-K1	Chinese hamster ovary K1 cells
NHE3	Na^+-H^+ exchanger 3
NKA	Na^+-K^+-ATPase
ENaC	epithelial Na^+ channel
PMA	phorbol-12-myristate-13-acetate
EGF	epidermal growth factor
α-CD	α-cyclodextrin
SGLT1	sodium glucose co-transporter 1
TEA	tetraethyl-ammonium bromide
HEK-293	human embryonic kidney 293 cells

References

1. Cohen AW, Hnasko R, Schubert W, Lisanti MP. Role of caveolae and caveolins in health and disease. Physiol Rev. 2004; 84:1341–1379. [PubMed: 15383654]
2. Simons K, Ikonen E. Functional rafts in cell membranes. Nature. 1997; 387:569–572. [PubMed: 9177342]
3. Cohen AW, Combs TP, Scherer PE, Lisanti MP. Role of caveolin and caveolae in insulin signaling and diabetes. Am J Physiol Endocrinol Metab. 2003; 285:E1151–E1160. [PubMed: 14607781]
4. Williams TM, Lisanti MP. The caveolin proteins. Genome Biol. 2004; 5:214. [PubMed: 15003112]
5. Li S, Song KS, Lisanti MP. Expression and characterization of recombinant caveolin. Purification by polyhistidine tagging and cholesterol-dependent incorporation into defined lipid membranes. J Biol Chem. 1996; 271:568–573. [PubMed: 8550621]
6. Murata M, Peranen J, Schreiner R, Wieland F, Kurzchalia TV, Simons K. Vip21/caveolin is a cholesterol-binding protein. Proc Natl Acad Sci U S A. 1995; 92:10339–10343. [PubMed: 7479780]
7. Smart EJ, Ying Y, Donzell WC, Anderson RG. A role for caveolin in transport of cholesterol from endoplasmic reticulum to plasma membrane. J Biol Chem. 1996; 271:29427–29435. [PubMed: 8910609]
8. Lockwich TP, Liu X, Singh BB, Jadlowiec J, Weiland S, Ambudkar IS. Assembly of trp1 in a signaling complex associated with caveolin-scaffolding lipid raft domains. J Biol Chem. 2000; 275:11934–11942. [PubMed: 10766822]
9. Syme CA, Zhang L, Bisello A. Caveolin-1 regulates cellular trafficking and function of the glucagon-like peptide 1 receptor. Mol Endocrinol. 2006; 20:3400–3411. [PubMed: 16931572]
10. Dhungana S, Merrick BA, Tomer KB, Fessler MB. Quantitative proteomics analysis of macrophage rafts reveals compartmentalized activation of the proteasome and of proteasome-mediated erk activation in response to lipopolysaccharide. Mol Cell Proteomics. 2009; 8:201–213. [PubMed: 18815123]

NIH-PA Author Manuscript

NIH-PA Author Manuscript

NIH-PA Author Manuscript

11. Chichili GR, Rodgers W. Cytoskeleton-membrane interactions in membrane raft structure. Cell Mol Life Sci. 2009; 66:2319–2328. [PubMed: 19370312]
12. Mundy DI, Machleidt T, Ying Y-s, Anderson RGW, Bloom GS. Dual control of caveolar membrane traffic by microtubules and the actin cytoskeleton. J Cell Sci. 2002; 115:4327–4339. [PubMed: 12376564]
13. Chichili GR, Rodgers W. Clustering of membrane raft proteins by the actin cytoskeleton. J Biol Chem. 2007; 282:36682–36691. [PubMed: 17947241]
14. Liu X, Mitrovic AD, Vandenberg RJ. Glycine transporter 1 associates with cholesterol-rich membrane raft microdomains. Biochem Biophys Res Commun. 2009; 384:530–534. [PubMed: 19427831]
15. Murtazina R, Kovbasnjuk O, Donowitz M, Li X. Na^+/H^+ exchanger nhe3 activity and trafficking are lipid raft-dependent. J Biol Chem. 2006; 281:17845–17855. [PubMed: 16648141]
16. Welker P, Geist B, Fruhauf JH, Salanova M, Groneberg DA, Krause E, Bachmann S. Role of lipid rafts in membrane delivery of renal epithelial Na^+-K^+-atpase, thick ascending limb. Am J Physiol Regul Integr Comp Physiol. 2007; 292:R1328–R1337. [PubMed: 17082358]
17. Kwak JO, Kim HW, Oh KJ, Kim DS, Han KO, Cha SH. Co-localization and interaction of organic anion transporter 1 with caveolin-2 in rat kidney. Exp Mol Med. 2005; 37:204–212. [PubMed: 16000875]
18. Kwak JO, Kim HW, Song JH, Kim MJ, Park HS, Hyun DK, Kim DS, Cha SH. Evidence for rat organic anion transporter 3 association with caveolin-1 in rat kidney. IUBMB Life. 2005; 57:109–117. [PubMed: 16036570]
19. Hilgendorf C, Ahlin G, Seithel A, Artursson P, Ungell A-L, Karlsson J. Expression of thirty-six drug transporter genes in human intestine, liver, kidney, and organotypic cell lines. Drug Metab Dispos. 2007; 35:1333–1340. [PubMed: 17496207]
20. Berkhin EB, Humphreys MH. Regulation of renal tubular secretion of organic compounds. Kidney Int. 2001; 59:17–30. [PubMed: 11135053]
21. Burckhardt BC, Burckhardt G. Transport of organic anions across the basolateral membrane of proximal tubule cells. Rev Physiol Biochem Pharmacol. 2003; 146:95–158. [PubMed: 12605306]
22. Dresser MJ, Leabman MK, Giacomini KM. Transporters involved in the elimination of drugs in the kidney: Organic anion transporters and organic cation transporters. J Pharm Sci. 2001; 90:397–421. [PubMed: 11170032]
23. Rizwan AN, Burckhardt G. Organic anion transporters of the slc22 family: Biopharmaceutical, physiological, and pathological roles. Pharm Res. 2007; 24:450–470. [PubMed: 17245646]
24. Kikuchi R, Kusuhara H, Sugiyama D, Sugiyama Y. Contribution of organic anion transporter 3 (slc22a8) to the elimination of p-aminohippuric acid and benzylpenicillin across the blood-brain barrier. J Pharmacol Exp Ther. 2003; 306:51–58. [PubMed: 12684544]
25. Ohtsuki S, Kikkawa T, Mori S, Hori S, Takanaga H, Otagiri M, Terasaki T. Mouse reduced in osteosclerosis transporter functions as an organic anion transporter 3 and is localized at abluminal membrane of blood-brain barrier. J Pharmacol Exp Ther. 2004; 309:1273–1281. [PubMed: 14762099]
26. Sweet DH, Chan LM, Walden R, Yang XP, Miller DS, Pritchard JB. Organic anion transporter 3 (slc22a8) is a dicarboxylate exchanger indirectly coupled to the Na^+ gradient. Am J Physiol Renal Physiol. 2003; 284:F763–F769. [PubMed: 12488248]
27. Sweet DH, Miller DS, Pritchard JB, Fujiwara Y, Beier DR, Nigam SK. Impaired organic anion transport in kidney and choroid plexus of organic anion transporter 3 (oat3 (slc22a8)) knockout mice. J Biol Chem. 2002; 277:26934–26943. [PubMed: 12011098]
28. Soodvilai S, Chatsudthipong V, Evans KK, Wright SH, Dantzler WH. Acute regulation of oat3-mediated estrone sulfate transport in isolated rabbit renal proximal tubules. Am J Physiol Renal Physiol. 2004; 287:F1021–F1029. [PubMed: 15238352]
29. Wolff NA, Thies K, Kuhnke N, Reid G, Friedrich B, Lang F, Burckhardt G. Protein kinase c activation downregulates human organic anion transporter 1-mediated transport through carrier internalization. J Am Soc Nephrol. 2003; 14:1959–1968. [PubMed: 12874449]

NIH-PA Author Manuscript

NIH-PA Author Manuscript

NIH-PA Author Manuscript

30. Barros SA, Srimaroeng C, Perry JL, Walden R, Dembla-Rajpal N, Sweet DH, Pritchard JB. Activation of protein kinase c zeta increases oat1 (slc22a6) and oat3 (slc22a8)-mediated transport. J Biol Chem. 2009; 284:2672–2679. [PubMed: 19028678]

31. Vanwert AL, Srimaroeng C, Sweet DH. Organic anion transporter 3 (oat3/slc22a8) interacts with carboxyfluoroquinolones, and deletion increases systemic exposure to ciprofloxacin. Mol Pharmacol. 2008; 74:122–131. [PubMed: 18381565]

32. Kirkham M, Parton RG. Clathrin-independent endocytosis: New insights into caveolae and non-caveolar lipid raft carriers. Biochim Biophys Acta. 2005; 1745:273–286. [PubMed: 16046009]

33. Okamoto T, Schlegel A, Scherer PE, Lisanti MP. Caveolins, a family of scaffolding proteins for organizing “preassembled signaling complexes” at the plasma membrane. J Biol Chem. 1998; 273:5419–5422. [PubMed: 9488658]

34. Gustavsson J, Parpal S, Karlsson M, Ramsing C, Thorn H, Borg M, Lindroth M, Peterson KH, Magnusson KE, Stralfors P. Localization of the insulin receptor in caveolae of adipocyte plasma membrane. Faseb J. 1999; 13:1961–1971. [PubMed: 10544179]

35. Ma DW. Lipid mediators in membrane rafts are important determinants of human health and disease. Appl Physiol Nutr Metab. 2007; 32:341–350. [PubMed: 17510668]

36. Schroer TA. Motors, clutches and brakes for membrane traffic: A commemorative review in honor of thomas kreis. Traffic. 2000; 1:3–10. [PubMed: 11208053]

37. Krueger B, Haerteis S, Yang L, Hartner A, Rauh R, Korbmacher C, Diakov A. Cholesterol depletion of the plasma membrane prevents activation of the epithelial sodium channel (enac) by sgk1. Cell Physiol Biochem. 2009; 24:605–618. [PubMed: 19910701]

38. Hong M, Xu W, Yoshida T, Tanaka K, Wolff DJ, Zhou F, Inouye M, You G. Human organic anion transporter hoat1 forms homooligomers. J Biol Chem. 2005; 280:32285–32290. [PubMed: 16046403]

39. Kojima R, Sekine T, Kawachi M, Cha SH, Suzuki Y, Endou H. Immunolocalization of multispecific organic anion transporters, oat1, oat2, and oat3, in rat kidney. J Am Soc Nephrol. 2002; 13:848–857. [PubMed: 11912243]

40. Srimaroeng C, Perry JL, Pritchard JB. Physiology, structure, and regulation of the cloned organic anion transporters. Xenobiotica. 2008; 38:889–935. [PubMed: 18668434]

41. Miller DS, Pritchard JB. Nocodazole inhibition of organic anion secretion in teleost renal proximal tubules. Am J Physiol. 1994; 267:R695–R704. [PubMed: 8092313]

42. Crljen V, Sabolic I, Susac J, Appenroth D, Herak-Kramberger CM, Ljubojevic M, Anzai N, Antolovic R, Burckhardt G, Fleck C, Sabolic I. Immunocytochemical characterization of the incubated rat renal cortical slices. Pflugers Arch. 2005; 450:269–279. [PubMed: 15895249]

43. You G, Kuze K, Kohanski RA, Amsler K, Henderson S. Regulation of moat-mediated organic anion transport by okadaic acid and protein kinase c in llc-pk(1) cells. J Biol Chem. 2000; 275:10278–10284. [PubMed: 10744714]

44. Duan P, Li S, You G. Angiotensin ii inhibits activity of human organic anion transporter 3 through activation of protein kinase calpha: Accelerating endocytosis of the transporter. Eur J Pharmacol. 2009; 627:49–55. [PubMed: 19878671]

45. Zhang Q, Suh W, Pan Z, You G. Short-term and long-term effects of protein kinase c on the trafficking and stability of human organic anion transporter 3. Int J Biochem Mol Biol. 2012; 3:242–249. [PubMed: 22773962]

46. Kilsdonk EP, Yancey PG, Stoudt GW, Bangerter FW, Johnson WJ, Phillips MC, Rothblat GH. Cellular cholesterol efflux mediated by cyclodextrins. J Biol Chem. 1995; 270:17250–17256. [PubMed: 7615524]

47. Saksena S, Tyagi S, Goyal S, Gill RK, Alrefai WA, Ramaswamy K, Dudeja PK. Stimulation of apical cl/hco(oh) exchanger, slc26a3 by neuropeptide y is lipid raft dependent. Am J Physiol Gastrointest Liver Physiol. 2000; 299:G1334–G1343. [PubMed: 20884887]

48. Thomsen P, Roepstorff K, Stahlhut M, van Deurs B. Caveolae are highly immobile plasma membrane microdomains, which are not involved in constitutive endocytic trafficking. Mol Biol Cell. 2002; 13:238–250. [PubMed: 11809836]

NIH-PA Author Manuscript
NIH-PA Author Manuscript
NIH-PA Author Manuscript

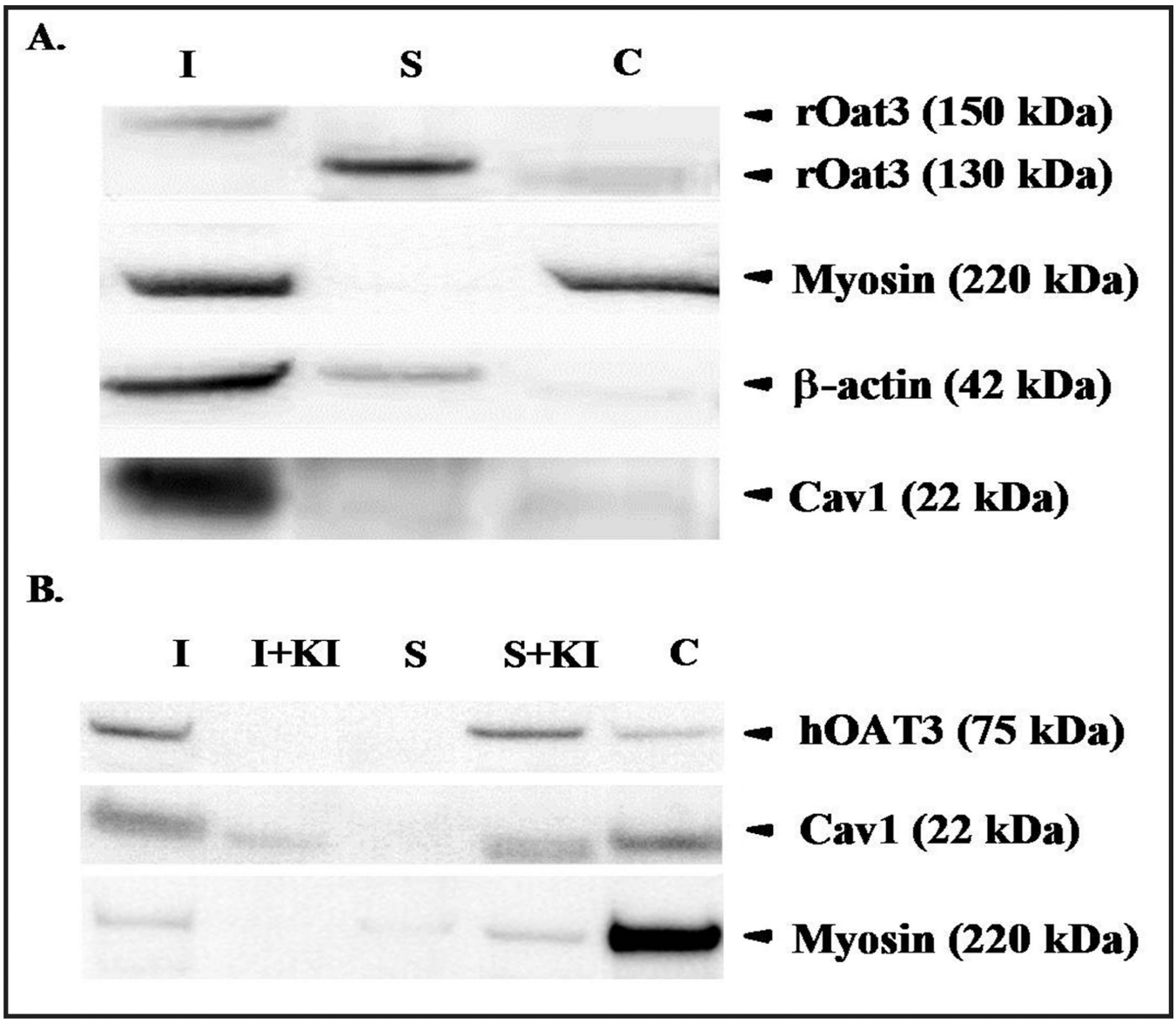

Fig. 1.

Distribution of human and rat Oat3 in cellular or tissue fractions. (A) Western blot detection of rOat3 as well as other cytoskeletal or LRD associated proteins in three cellular fractions or rat renal cortex. Fractions are designated: Insoluble (I), Soluble (S) and Cytosolic (C) (B) Relative presence of hOAT3, Cav1 and myosin in cellular fractions (using fraction designations described in 1A) from HEK-293 cells. Two additional fractions were probed for hOAT3, Cav1 and myosin quantities after the addition of the cytoskeletal disruptor; KI was added (shown as S + KI and I + KI). Representative data from one of at least three separate experiments is shown.

NIH-PA Author Manuscript
NIH-PA Author Manuscript
NIH-PA Author Manuscript

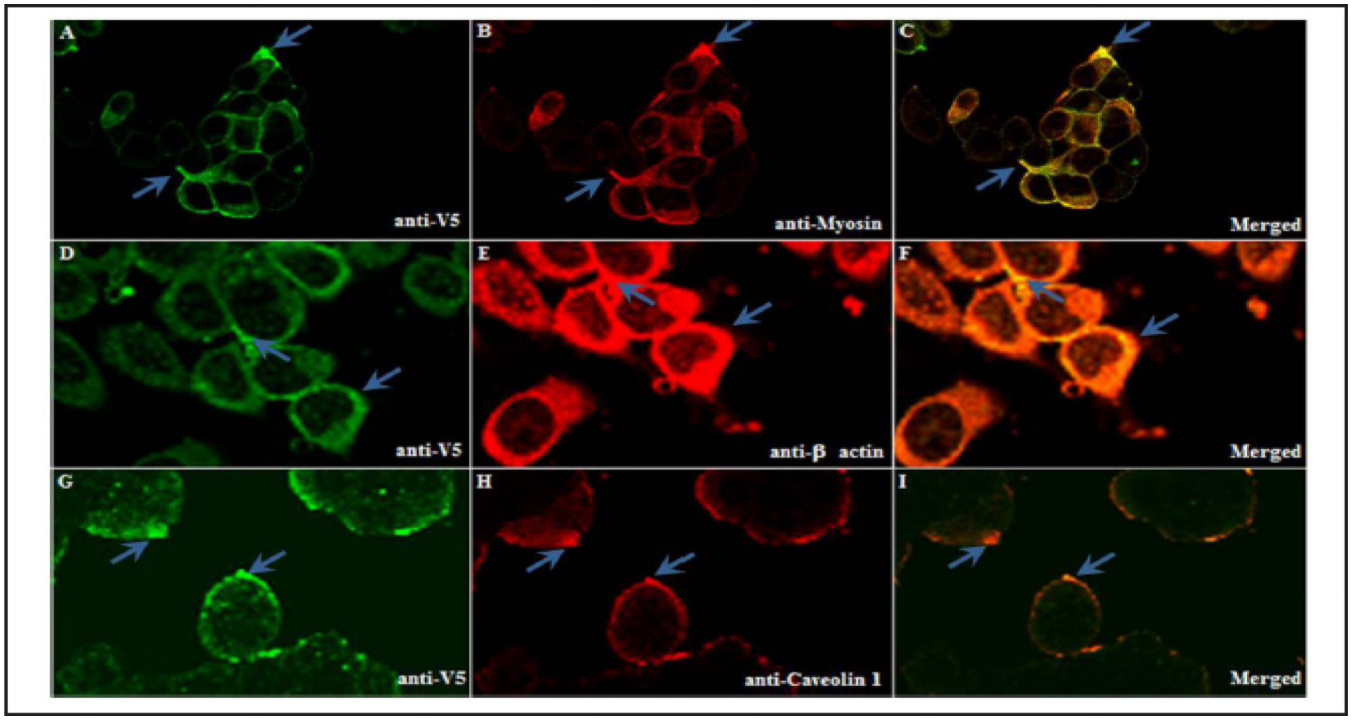

Fig. 2.

Human OAT3 and LRD associated proteins co-localized on the plasma membrane of HEK-293 cells. HEK-293 cells transfected with hOAT3-V5 tag were seeded, fixed, permeabilized and stained with a primary antibody against the V5 tag (A, D, G). Additional LRD proteins were stained using antibodies against myosin (B), β-actin (E) and Cav1 (H). Localization was probed with either anti-mouse and/or anti-rabbit fluorescent secondary antibody by laser scanning confocal microscopy. Images C, F, and I were overlay images of A–B, D–E, and G–H, respectively. Representative data from one of at least three separate experiments is shown.

NIH-PA Author Manuscript

NIH-PA Author Manuscript

NIH-PA Author Manuscript

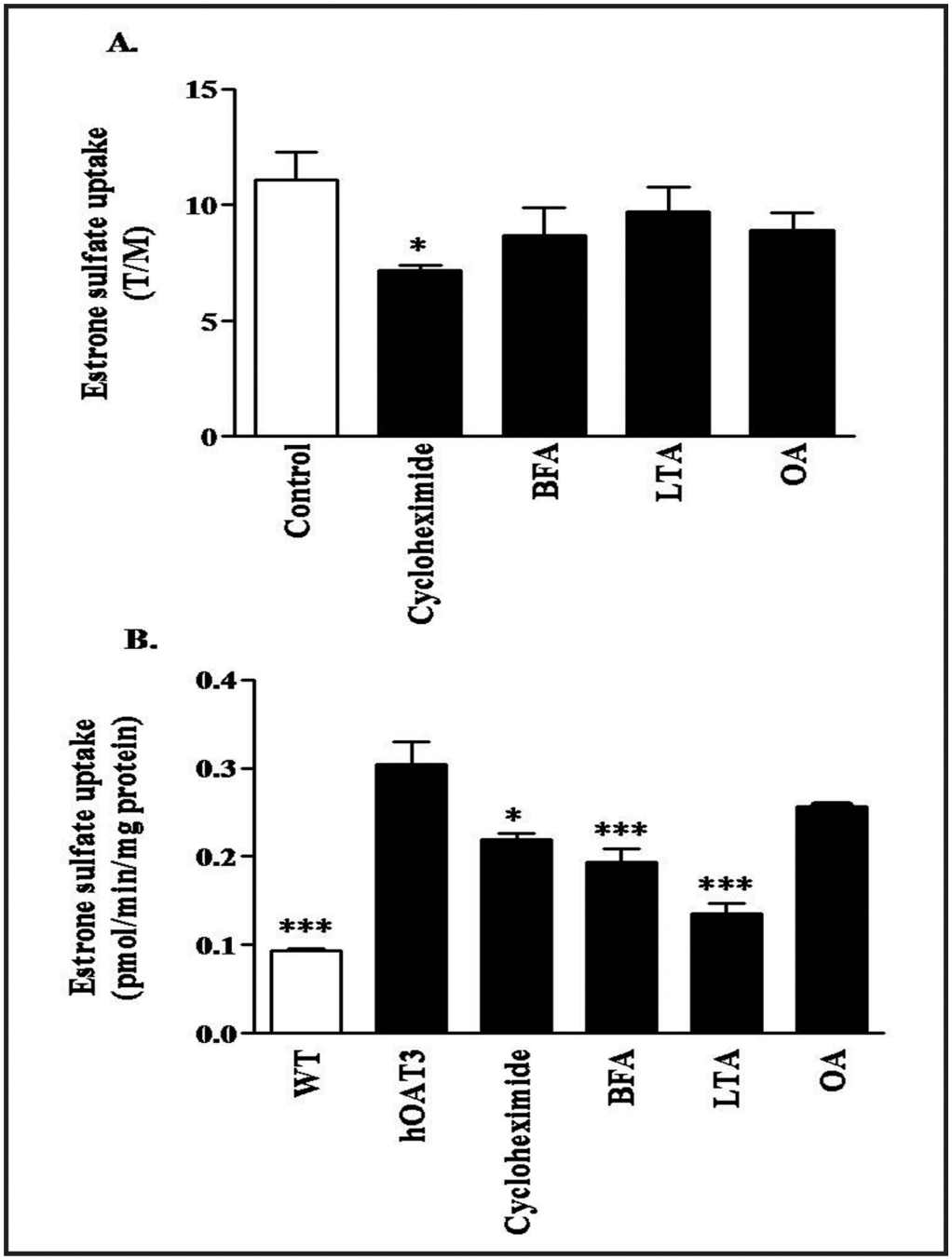

Fig. 3.

Effect of cytoskeletal disruptors on ES uptake mediated by Oat3. (A) Rat renal cortical slices were pre-incubated with buffer or with buffer containing 50 μM cycloheximide, 50 μg/ml brefeldin A (BFA), 50 μM latrunculin A (LTA), and 1 μM okadaic acid (OA) for 30 min. [^{3}H]-ES at 100 nM was subsequently added and slices were incubated for 30 min at room temperature. Uptake of [^{3}H]-ES was measured, and tissue to medium ratios (T/M) were determined as described in the experimental section. Each experiment was conducted three times from 3–4 animals. (B) HEK-293 cells stably expressing hOAT3 were pre-incubated with buffer or buffer containing test compounds as mentioned above in Figure 3A for 30 min. Uptake of [^{3}H]-ES was determined after 5 min and is shown as pmol/min/mg

protein. Each experiment was conducted three times from 3–4 animals. *p<0.05 or ***p<0.001 indicates significant differences from the slices or HEK-293 expressed hOAT3 cells incubated with cytoskeletal disruptors or protein trafficking inhibitors versus with buffer alone. WT: wild type HEK-293 cells.

NIH-PA Author Manuscript
NIH-PA Author Manuscript
NIH-PA Author Manuscript

NIH-PA Author Manuscript

NIH-PA Author Manuscript

NIH-PA Author Manuscript

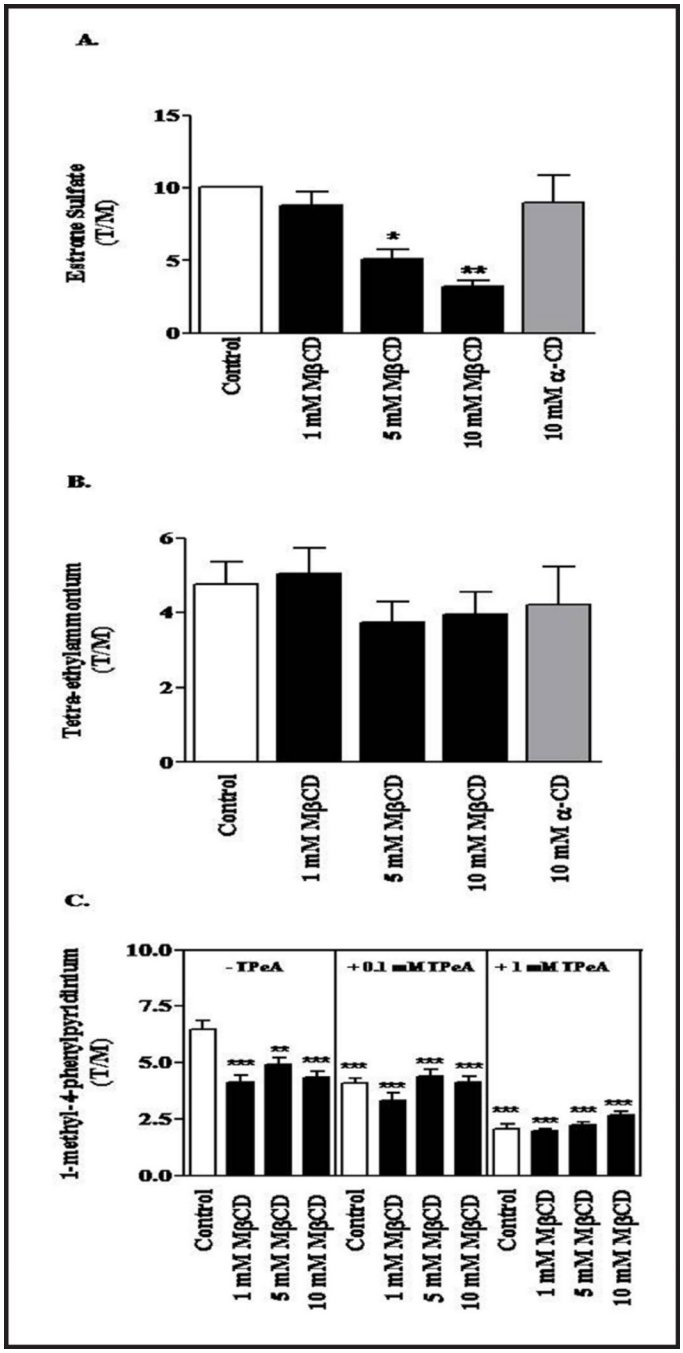

Fig. 4.

Effect of cholesterol depletion on the transport of substrates by rOat3 and rOcts. (A) To test the function of rOat3, rat renal cortical slices were pre-incubated with buffer or with buffer containing 1, 5 or 10 mM MβCD or 10 mM α-CD for 30 min. Subsequently, the tissue slices were treated with 100 nM [^{3}H]-ES for 30 additional min. (B) To test the function of rOcts, rat renal cortical slices were incubated with buffer or with buffer containing 1, 5 or 10 mM MβCD or 10 mM α-CD for 30 min. Tissue slices were then incubated in the presence of the radiolabeled OCT substrate, [^{3}H]-TEA, at a concentration of 10 μM for 30 min. (C) To test tetra-pentylammomium (TPeA)-sensitive MPP^+ uptake mediated by rOcts, rat renal cortical slices were incubated with buffer alone or with buffer containing 1, 5 or 10 mM MβCD for

NIH-PA Author Manuscript

NIH-PA Author Manuscript

NIH-PA Author Manuscript

30 min (left panel). Renal tissue slices were then incubated in the presence or absence of 100 μM (middle panel) or 1 mM (right panel) of TPeA, and all samples were subsequently incubated in buffer containing 1 nM of [^{3}H]-MPP$^+$ for 30 min. The radiolabeled substrates were measured and calculated as tissue to medium ratios (T/M), were determined as described in the experimental section. Each experiment was conducted from separate animals (n = 3–5). *$p<0.05$, **$p<0.01$ or ***$p<0.001$ indicates significant differences from the slices incubated with buffer alone.

NIH-PA Author Manuscript

NIH-PA Author Manuscript

NIH-PA Author Manuscript

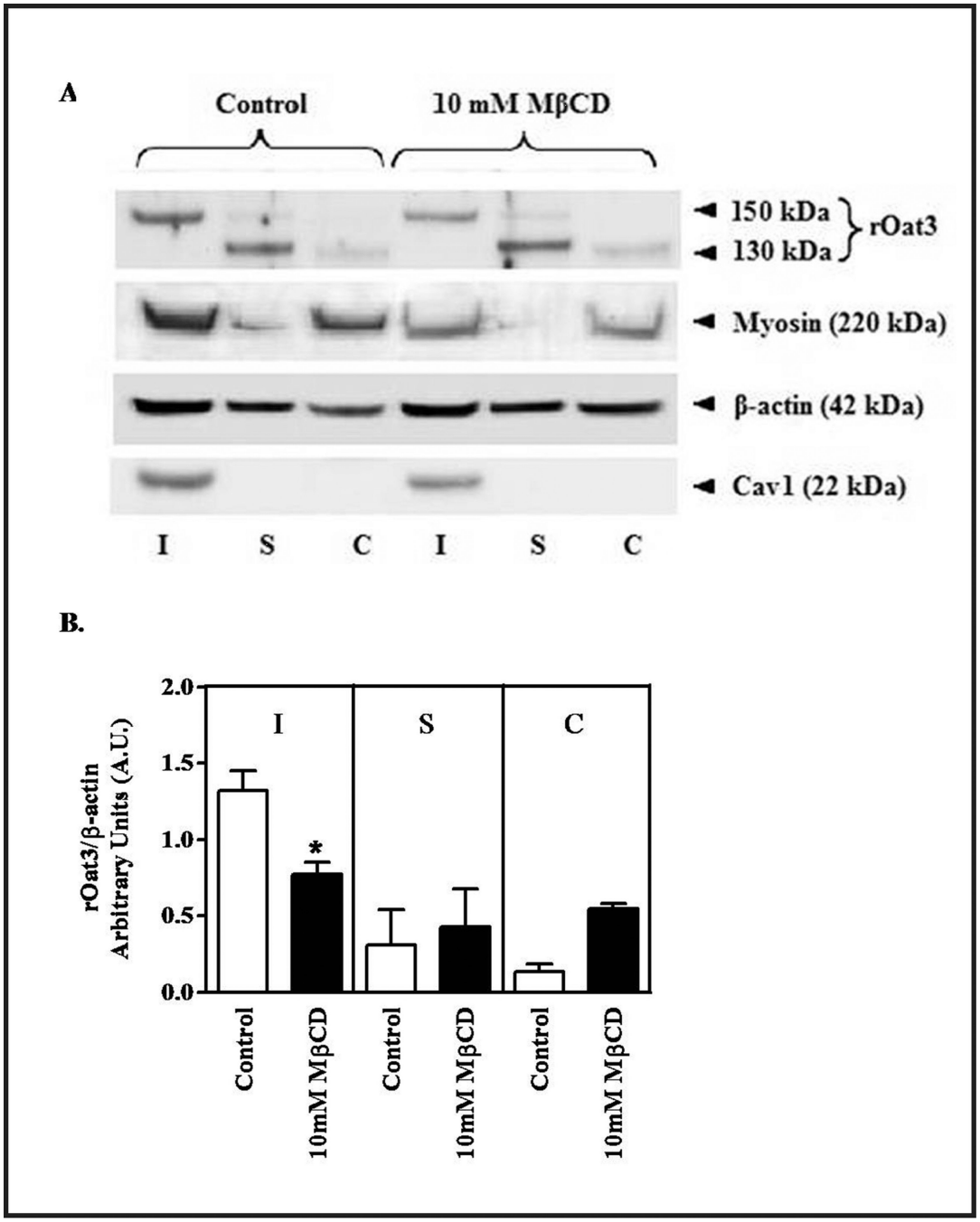

Fig. 5.

Effect of cholesterol depletion on the expression of rOat3 and LRD associated proteins. (A) Rat renal cortical slices were pre-incubated in the presence of buffer or with buffer containing 10 mM MβCD for 30 min. Three tissue fractions were prepared as insoluble (I, the LRD-rich membrane region), soluble (S, the non-LRD-rich membrane region) and cytosolic (C). Following gel electrophoresis and Western blotting, the relative expression of proteins in each fraction was observed using antibodies against rOat3 and LRD associated proteins as described in the experimental section. Experiments were conducted for three times and a representative Western blot is shown. (B) The relative abundance of rOat3 and β-actin in each fraction and treatment was quantified with densitometry. The amount of

rOat3 in control and MβCD treated samples was normalized by the amount of β-actin present. Mean results from three separate experiments appear as a ratio of the respective densities (rOat3/β-actin). *p<0.05 indicates significant differences in rOat3 protein expression in the presence of 10 mM MβCD.

NIH-PA Author Manuscript
NIH-PA Author Manuscript
NIH-PA Author Manuscript

NIH-PA Author Manuscript
NIH-PA Author Manuscript
NIH-PA Author Manuscript

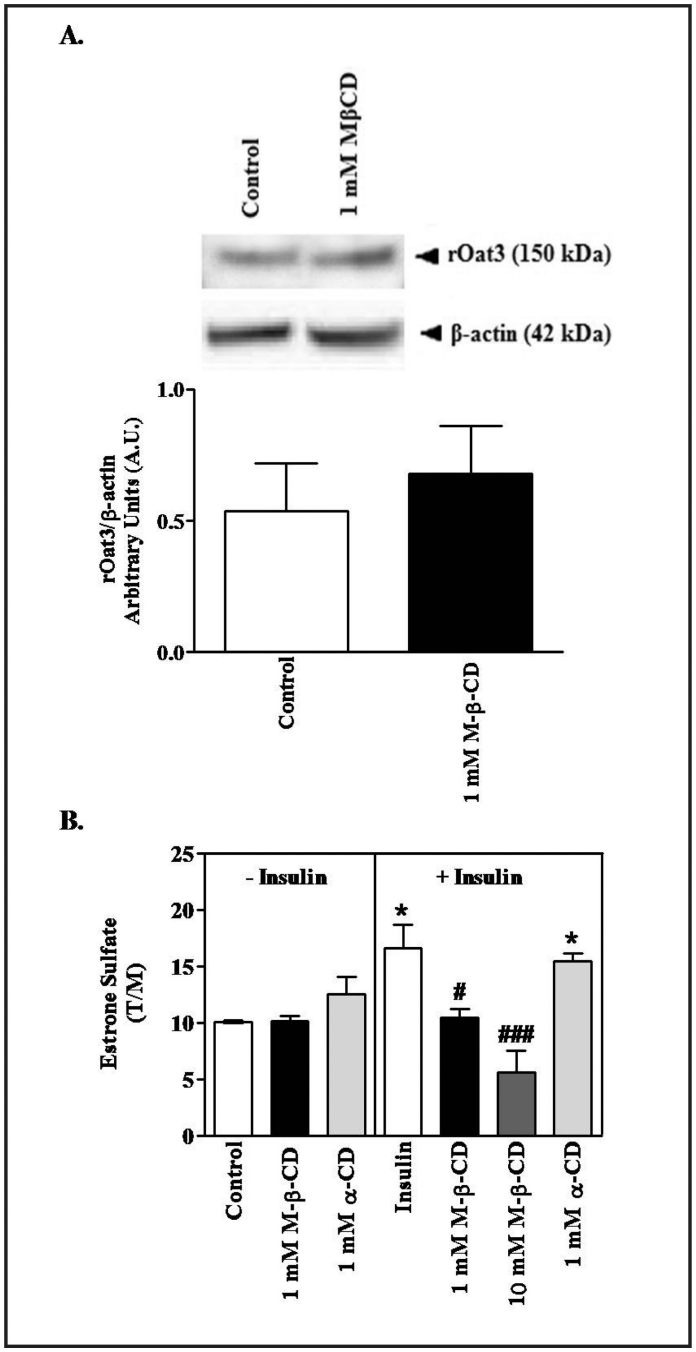

Fig. 6.

Effect of cholesterol depletion on insulin stimulated ES transport by rOat3. (A) Upper panel: Rat renal cortical slices were pre-incubated in the presence of buffer or with buffer containing 1 mM MβCD for 30 min. Three fractions were prepared as mentioned above in Figure 5A. Following gel electrophoresis and Western blotting, the relative expression of rOat3 and β-actin in the LRD-rich fraction was observed with antibody detection as described in the experimental section. Experiments were conducted for three times and a representative Western blot is shown. Lower panel: The relative abundance of rOat3 and β-actin in the LRD-rich fraction and treatment was quantified with densitometry. The amount of rOat3 in control and MβCD treated samples was normalized by the amount of β-actin

NIH-PA Author Manuscript

NIH-PA Author Manuscript

NIH-PA Author Manuscript

present. Mean results from three separate experiments appear as a ratio of the respective densities (rOAT3/β-actin). (B) Rat renal cortical slices were pre-incubated with buffer, 1 mM MβCD, or 1 mM α-CD in the presence or absence of 30 μg/ml insulin for 30 min. Subsequently, the samples were incubated in 100 nM of [^{3}H]-ES for 30 min. Uptake of [^{3}H]-ES was measured and tissue to medium ratios (T/M), were determined as described in the experimental section. Means from three separate experiments (n= 3–4 animals) are shown. *p<0.05 indicates significant differences from the control (tissue slices incubated with buffer followed by uptake of ES); $^{\#}p$<0.05, $^{\#\#\#}$p<0.001 indicates significant differences from the tissue slices incubated with buffer in the presence of insulin followed by uptake of ES.